CDDpress

www.nature.com/cdd

ARTICLE

Check for updates

SIRT5-mediated ME2 desuccinylation promotes cancer growth by enhancing mitochondrial respiration

Peng Teng[1,2], Kaisa Cui[1,2], Surui Yao[1,2], Bojian Fei[2,3], Feng Ling[4], Chaoqun Li[1,2]✉ and Zhaohui Huang[1,2]✉

Mitochondrial malic enzyme 2 (ME2), which catalyzes the conversion of malate to pyruvate, is frequently upregulated during tumorigenesis and is a potential target for cancer therapy. However, the regulatory mechanism underlying ME2 activity is largely unknown. In this study, we demonstrate that ME2 is highly expressed in human colorectal cancer (CRC) tissues, and that ME2 knockdown inhibits the proliferation of CRC cells. Furthermore, we reveal that ME2 is succinylated and identify Sirtuins 5 (SIRT5) as an ME2 desuccinylase. Glutamine deprivation directly enhances the interaction of SIRT5 with ME2 and thus promotes SIRT5-mediated desuccinylation of ME2 at lysine 346, activating ME2 enzymatic activity. Activated ME2 significantly enhances mitochondrial respiration, thereby counteracting the effects of glutamine deprivation and supporting cell proliferation and tumorigenesis. Additionally, the levels of succinylated ME2 at K346 and SIRT5 in CRC tissues, which are negatively correlated, are associated with patient prognosis. These observations suggest that SIRT5-catalyzed ME2 desuccinylation is a key signaling event through which cancer cells maintain mitochondrial respiration and promote CRC progression under glutamine deficiency conditions, offering the possibility of targeting SIRT5-mediated ME2 desuccinylation for CRC treatment.

Cell Death & Differentiation (2024) 31:65–77; https://doi.org/10.1038/s41418-023-01240-y

INTRODUCTION

Metabolism reprogramming is a hallmark of cancer [1]. Rapid tumor cell proliferation highly depends on the reprogramming of aerobic glycolysis, mitochondrial respiration, glutamic acidolysis, and lipid metabolism [1, 2]. Previously, it was thought that the heavy reliance of cancer cells on glycolysis was due to mitochondrial dysfunction [3, 4]. However, recent studies have shown that mitochondrial respiration is also utilized by cancer cells to fulfill the requirements for proliferation [5–8]. Cancer cells usually exhibit enhanced mitochondrial metabolism, which is essential for redox maintenance, biosynthetic and bioenergetic processes [9, 10]. Previous studies have revealed that strengthened oxidative phosphorylation (OXPHOS) contributes to cancer progression, and some OXPHOS-related enzymes are generally highly expressed in human cancers, including colorectal cancer (CRC) [11–13]. However, it remains unclear how these enzymes are regulated and whether they are involved in the occurrence and development of cancers. In particular, the tumor metabolic microenvironment is characterized by the fluctuating or limited availability of nutrients and mitochondrial metabolism has been reported to contribute to the adaptation of tumor cells to nutrient-deficient environments. Nevertheless, the molecular mechanisms underlying how cancer cells sense nutrient signals and coordinate nutrient levels to metabolic flux through mitochondrial enzymes have not been fully elucidated.

Malic enzymes (MEs) catalyze the oxidative decarboxylation of malate to generate pyruvate and either NADPH or NADH with $NAD(P)^+$ functioning as a coenzyme. In mammalian cells, there are three isoforms of MEs, including a cytosolic $NADP^+$-dependent isoform (ME1), a mitochondrial $NAD(P)^+$-dependent isoform (ME2), and a mitochondrial NAD^+-dependent isoform (ME3). Compared with that of ME3, the content of ME2 is higher in cells, and ME2 plays a more important regulatory role in cell metabolism. ME2 regulates TCA flux in response to cellular demands for energy, carbon skeletons, and reducing equivalents [14, 15]. In addition, ME2 significantly enhances glutamine and lipid metabolism in cancer cells, thereby meeting their high metabolic demand [14]. Aberrant ME2 expression has been found in a variety of cancers, and 2-hydroxyglutarate (2-HG) generated by ME2 is involved in the stabilization of mutant p53 and CRC tumor growth [15–17], while α-ketoglutarate (α-KG) produced by ME2 promotes cell cycle progression by upregulating the transcription of cyclin D1 [18]. However, little is known about the mechanism regulating the activity of ME2.

In the past decade, post-translational modifications (PTM) of proteins, especially those of metabolic enzymes, have attracted considerable attention and have led to a deeper understanding of the role of cell metabolism in human diseases, especially cancers. Succinylation refers to the addition of succinyl coenzyme A to the lysine side chain of a protein, thereby altering its structure and function. Compared to the effects of other PTM types, succinylation usually causes greater changes in the mass, spatial structure, and charge properties of the modified protein, therefore, succinylation generally exerts a greater regulatory effect on protein functions [19]. It has been reported that succinylation can affect the localization, trafficking, stability, activity, and

[1]Wuxi Cancer Institute, Affiliated Hospital of Jiangnan University, Wuxi 214062 Jiangsu, China. [2]Laboratory of Cancer Epigenetics, Wuxi School of Medicine, Jiangnan University, Wuxi 214062 Jiangsu, China. [3]Department of General Surgery, Affiliated Hospital of Jiangnan University, Wuxi 214062 Jiangsu, China. [4]Chemical Genetics Laboratory, RIKEN Advanced Science Institute, Hirosawa 2-1, Wako-shi, Saitama 351-0198, Japan. ✉email: licq@jiangnan.edu.cn; zhaohuihuang@jiangnan.edu.cn

Received: 7 August 2023 Revised: 31 October 2023 Accepted: 7 November 2023
Published online: 25 November 2023

signaling of target proteins, thus differentiating the metabolism of tumor cells from that of normal cells and influencing tumorigenesis [19–21]. However, whether ME2 is regulated by succinylation to support tumor growth remains unclear.

In this study, we demonstrate that ME2 is highly expressed in CRC tissues and promotes tumor growth. ME2 desuccinylation at K346 mediated by Sirtuins 5 (SIRT5) increases its activity. Glutamine starvation enhances the interaction of ME2 with SIRT5, leading to the desuccinylation and activation of ME2. Activated ME2 significantly enhances mitochondrial respiration to counteract glutamine starvation and promote tumor cell survival and proliferation.

RESULTS

ME2 is overexpressed in CRC and promotes CRC proliferation

First, we analyzed the mRNA expression of ME2 based on the TCGA dataset and found that ME2 was overexpressed in most digestive tract tumors (Fig. 1A). The upregulation of ME2 mRNA levels in CRC was further validated in a GEO database (GSE73360, Fig. 1B). To confirm the overexpression of ME2 in CRC cells, we detected the ME2 protein levels in 10 paired CRC tissues using western blotting, and observed increased expression of ME2 in 6 cases (Fig. 1C). Furthermore, we analyzed ME2 protein expression in 146 paired CRC tissues by immunohistochemistry (IHC) staining and found that the expression of ME2 was elevated in more than one-half of the CRC samples (50.68%, 74/146) compared with matched noncancerous tissues (NCTs) ($P < 0.001$, Fig. 1D; Fig. S1), and patients with higher ME2 expression exhibited poorer overall survival (Fig. 1E). Statistical analyses revealed that ME2 expression in CRC tissues was positively correlated with tumor differentiation and stage (Table 1). In addition, both univariate and multivariate Cox proportional hazards analyses showed that ME2 was a prognostic factor for CRC patients (Fig. 1F). Together, these results indicate that ME2 expression is increased and correlates with a poor prognosis in CRC patients.

To determine whether ME2 promotes CRC cell proliferation, we depleted ME2 using small interfering RNA (siRNA) in HCT116, RKO, and Caco-2 cells, which exhibit relatively high ME2 expression (Fig. 1G, H), and observed that ME2 knockdown inhibited the proliferation in all these CRC cell lines (Fig. 1I). These results suggest that high ME2 expression is crucial to CRC cell proliferation.

SIRT5 interacts with and desuccinylates ME2

As an important metabolic enzyme in mitochondria, ME2 catalyzes the oxidative decarboxylation of malic acid to yield pyruvate and is essential for the maintenance of cellular NADPH levels [14, 22]. To explore the precise functions of ME2 in cellular metabolism, we overexpressed a Flag-tagged ME2 in HEK293T cells. These cells were then subjected to co-immunoprecipitation (co-IP), and mass spectrometry analyses performed to identify potential ME2-interacting proteins. Notably, SIRT5, the only known desuccinylase located in mitochondrion, was identified as a potential ME2-associated protein (Fig. 2A). In addition, immunofluorescence (IF) analyses showed the colocalization of ME2 and SIRT5 to mitochondria (Fig. 2B). The endogenous interaction of ME2 and SIRT5 was also confirmed using co-IP assays in HCT116 cells (Fig. 2C). Therefore, these data indicate that ME2 interacts with SIRT5.

Recent studies have shown that SIRT5 is involved in tumorigenesis through the desuccinylation of multiple metabolic enzymes [20, 23]. Therefore, we speculated that the existence of ME2 succinylation that is regulated by SIRT5. Using different amounts of succinyl-CoA, in vitro succinylation experiments showed that the succinylation levels of ME2 were increased in a dose-dependent manner (Fig. 2D). We next overexpressed ME2-Flag in HEK293T cells and treated these cells with the pan-sirtuin inhibitor nicotinamide (NAM) to suppress SIRT5 desuccinylase activity. The results showed that ME2 was indeed succinylated and that NAM treatment elevated its succinylation levels (Fig. 2E). In addition, the endogenous succinylation level of ME2 was also increased by NAM treatment in a time-dependent manner (Fig. 2F). These results enabled us to verify that SIRT5 dessuccinylates ME2. We confirmed that SIRT5 showed the greatest desuccinylation effects on ME2, while SIRT5 H158Y, a enzymatically defective SIRT5 mutant, failed to desuccinylate ME2 (Fig. 2G). Taken together, these data indicate that SIRT5 desuccinylates ME2.

CRC cells are highly dependent on glutamine [24]. Moreover, SIRT5 has also been reported to be closely related to glutamine metabolism and to promote CRC development by enhancing glutamine catabolism [23]. To evaluate whether SIRT5-mediated ME2 desuccinylation is regulated by glutamine availability, we cultured HEK293T cells cotransfected with Flag-tagged ME2 and HA-tagged SIRT5 in the presence or absence of glutamine. Interestingly, glutamine starvation significantly promoted the interaction between ME2 and SIRT5 (Fig. 2H). Additionally, the interaction of SIRT5 with ME2 facilitated by glutamine starvation was validated at the endogenous level in HCT116 cells (Fig. 2I**)**. Together, these results suggest that SIRT5 senses glutamine availability to dessuccinylate ME2.

ME2 is succinylated at K346

To identify potential succinylation sites on ME2, we purified the succinylated ME2 protein from HEK293T cells and determined its succinylation sites via mass spectrometry. Four potential succinylated lysine sites (K224, K240, K272, and K346) were identified in ME2 (Fig. 3A and S2). We next generated Arg (R, mimicking the desuccinylated state) and Glu (E, mimicking the negatively charged succinyllysine modification) substitution mutants of these sites and expressed these Flag-tagged ME2 mutants in HEK293T cells. Of these mutants, the K346R mutant showed obviously lower succinylation levels, indicating that K346 is the key succinylation site on ME2 (Fig. 3B). Moreover, sequence alignments showed that K346 of ME2 is a conserved residue among diverse species (Fig. 3C).

To confirm K346 succinylation in vivo, we generated an antibody that specifically recognized succinylated K346 on ME2. Dot blot assays showed that the anti-succ-K346 antibody preferentially recognized the K346-succinylated peptide but not the unsuccinylated control peptide (Fig. 3D), indicating good specificity of this generated antibody. Western blotting assays using this site-specific antibody detected a strong signal representing ectopically expressed wild-type (WT) ME2 and negligible levels of the K346R and K346E mutants (Fig. 3E). Indeed, NAM treatment increased the succinylation levels of ME2 K346 in a time-dependent manner (Fig. 3F). Succinylated K346 signal could be detected in both HEK293T and HCT116 cells **(**Fig. 3G, H), suggesting that K346 succinylation is a physiological PTM of ME2. Notably, the ME2 K346 succinylation levels were decreased in cells suffering from glutamine starvation (Fig. 3I). Next, we investigated whether SIRT5 is the desuccinylase that specifically mediates ME2 K346 desuccinylation. We observed that WT SIRT5, but not the SIRT5 H158Y mutant, decreased the ME2 K346 succinylation levels (Fig. 3J). Furthermore, siRNA-mediated knockdown of endogenous SIRT5 increased the ME2 K346 succinylation levels (Fig. 3K). To further characterize the clinical relevance of ME2 K346 succinylation, we examined ME2 K346 succinylation levels in CRC tissues by western blotting. The results showed that tumor samples displayed a less intense ME2 K346 succinylation signal than that of adjacent normal tissues (Fig. 3L). Taken together, these data suggest that K346 is the major succinylation site of ME2.

Desuccinylation at K346 by SIRT5 enhances ME2 activity

We next investigated the impact of succinylation on ME2 enzymatic activity. Specifically, cells treated with succinyl-CoA, which increased ME2 succinylation levels, showed reduced ME2

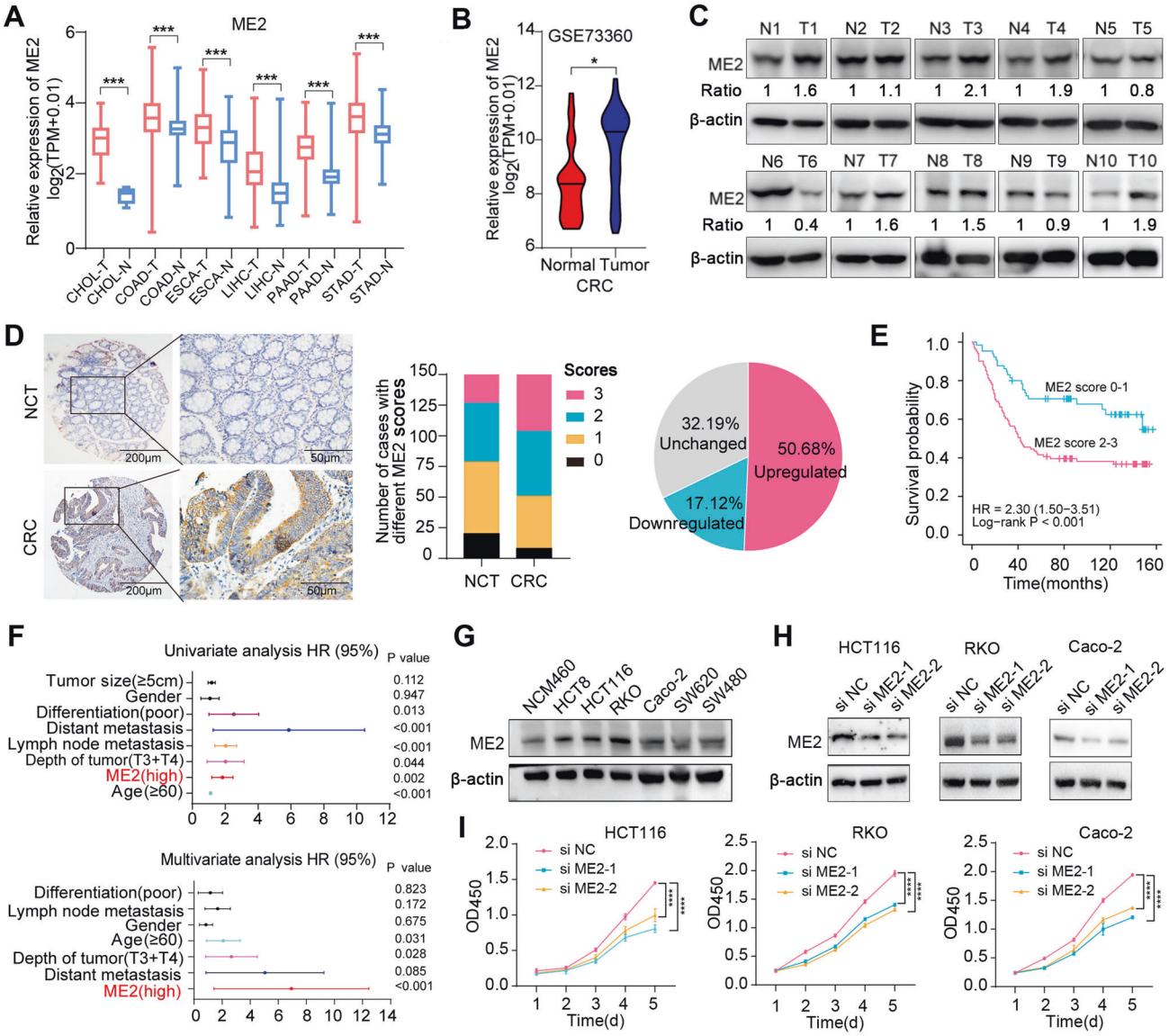

Fig. 1 ME2 is overexpressed in CRC cells and promotes their proliferation. A ME2 mRNA expression in digestive tract tumors and adjacent normal tissues from The Cancer Genome Atlas (TCGA) dataset. Mann-Whitney U Test was used for statistical analyses. **B** Relative mRNA expression levels of ME2 in the CRC dataset of GSE73360. **C** Detection and quantification of ME2 protein levels in 10 paired clinical CRC tissues (T) and adjacent normal tissues (N) by western blotting. **D** IHC analyses were performed with 146 paired tumor tissues and adjacent noncancerous tissues (NCT). **E** Kaplan-Meier survival analyses based on the expression of ME2 in CRC tissues. Patients with high ME2 expression (score 2-3) had poorer OS than those with low ME2 expression (score 0–1). *P* values were calculated using the log-rank test (Mantel-Cox). **F** Univariate and Multivariate Cox regression analyses. The hazard ratio (HR) and 95% confidence interval (CI) are plotted for each factor. **G** ME2 protein levels in CRC cell lines and the normal human colon cell line NCM460 were detected by western blotting. **H** Validation of the knockdown efficiency of ME2 in CRC cells transfected with ME2-specific short interfering RNAs (siME2) or control siRNA (siNC) using western blotting. **I** Effects of ME2 knockdown on CRC cell proliferation were evaluated by CCK-8 assays. The *P* values were determined by Dunnett's test after one-way ANOVA. Data are shown as mean ± S.D ($n = 3$). *, $p < 0.05$; ***, $p < 0.001$, ****, $p < 0.0001$.

activity (Fig. 4A). In addition, knockdown of SIRT5 increased ME2 succinylation levels and reduced ME2 activity (Fig. 4B). These data indicate that the enzymatic activity of ME2 is negatively correlated with its succinylation level, which is regulated by SIRT5.

Since K346 is the key succinylation site on ME2, we further evaluated whether K346 succinylation modulates ME2 enzymatic activity. We expressed Flag-tagged WT ME2 or ME2 mutants (K346R and K346E) in HEK293T cells and performed immunoprecipitaion and ME2 enzymatic activity assays. The activity of ME2 K346R was markedly elevated, whereas the activity of the K346E mutant was significantly reduced compared with that of WT ME2 (Fig. 4C). We also purified recombinant ME2 proteins (WT, K346R and K346E) to confirm the succinylation-regulated activity of ME2, and observed that the K346R mutant, but not the K346E mutant, showed enhanced activities compared with WT ME2 (Fig. 4D). Moreover, adding succinyl-CoA to the system increased the succinylation level of WT ME2 and decreased its enzyme activity, which was not observed when the ME2 K346E mutant was exposed to succinyl-CoA (Fig. 4E). Importantly, compared to WT ME2, both the succinylation levels and activities of the K346R and K346E mutants remained unchanged in response to altered glutamine levels, indicating that K346 is the major succinylation site on ME2 responding to glutamine starvation (Fig. 4F).

Considering that most mitochondrial proteins are reported to be acetylated [25], to exclude the effect of K346 acetylation on ME2 enzyme activity and function, we mutated this site to

Table 1. The relationship between ME2 protein levels and clinicalpathological parameters in CRC.

Characteristics	ME2		*P*
	Low	High	
Ages, y			
<60	32	40	0.611
≥60	36	38	
Gender			
Male	36	48	0.294
Female	32	30	
Tumor size (cm)			
<5	34	48	0.161
≥5	34	30	
Location			
Colon	30	42	0.241
Rectum	38	36	
Differentiation			
Well and moderately	50	45	0.045
Poorly	18	33	
Depth of tumor			
T1 + T2	21	15	0.166
T3	34	40	
T4	13	23	
Tumor stage			
I + II	44	30	0.002
III + IV	24	48	

Glutamine (Q, to mimic acetylated state) and failed to observe an obvious effect of K346Q on the enzymatic activity of ME2 (Fig. 4G). We then attempted to provide structural evidence to explain the effect of K346 succinylation on ME2 activity. The crystal structure of ME2 proteins revealed that K346 is in front of a critical channel involved in L-malate (substrate) and NAD^+ (coenzyme) entry, and positively charged amino acids may make it easier for acidic substrates to enter the active pocket. Because it simulates ME2 in the desuccinylated state, the surroundings of the ME2 K346R mutant became positively charged, thereby enhancing the ability of the mutant to bind NAD^+ and L-malate, whereas K346 bounded to the succinyl group (K346E, succinylated mimic) prevented NAD^+ and L-malate binding due to the negative charge of the lysine side chain (Fig. 4H), partially explaining how the succinylation at K346 regulates ME2 enzymatic activity. We further quantified the kinetic values of ME2 and its mutants with its substrates and coenzymes. Compared to WT ME2, the K346R mutant showed decreased Km values, whereas the K346E mutant showed increased Km values for NAD^+ and L-malate (Fig. 4I). Taken together, these results demonstrate that the succinylation at K346 regulates ME2 enzymatic activity.

ME2 K346 desuccinylation modulates mitochondrial respiration and redox homeostasis

ME2 catalyzes the conversion of malate to pyruvate, producing large amounts of NADPH which is closely related to energy metabolism and counteracts oxidative stress in tumor cells [26] (Fig. 5A). Recently, ME2 has been reported to sustain cell redox homeostasis in MYC-driven T-cell lymphoma [22]. To determine whether SIRT5-regulated desuccinylation of ME2 K346 affects mitochondrial metabolism and cellular redox homeostasis, we depleted the endogenous ME2, and simultaneously reconstituted it with short hairpin RNA (shRNA)-resistant Flag-tagged WT ME2, ME2 K346R or ME2 K346E in HCT116 cells (Fig. 5B). Consistent with previous reports [14], depletion of ME2 increased cellular ROS (reactive oxygen species) levels (Fig. 5C) and reduced the ratio of $NADPH/NADP^+$ (Fig. 5D), which were almost completely reversed by the reconstituted expression of WT ME2. Interestingly, the reconstituted expression of ME2 K346R, but not that of ME2 K346E, exhibited a stronger reversing effect than WT ME2 (Fig. 5C, D). In line with these results, depletion of ME2 reduced the ratio of GSH/oxidized glutathione (GSSG), and the reconstituted expression of WT ME2 mitigated this reduction (Fig. 5E). However, compared to cells with reconstituted expression of WT ME2, cells with the reconstituted expression of ME2 K346R, but not that of ME2 K346E, showed a higher GSH/GSSG ratio (Fig. 5E). Similarly, we detected the pyruvate and malate levels in these reconstituted HCT116 cells. After ME2 knockdown, pyruvate levels decreased, and malate levels increased, and these effects were fully reversed by the reconstituted expression of ME2 K346R but not ME2 K346E (Fig. 5F, G). Given that ME2 is related to lipid metabolism [14, 27], we also measured triglyceride levels and found that cells with reconstituted expression of ME2 K346R showed higher triglyceride levels (Fig. 5H). These results imply that the desuccinylation of ME2 K346 increases ME2 activity, which in turn contributes to cellular redox homeostasis and regulates the levels of related metabolites.

Considering that ME2 is a key regulatory enzyme of the TCA cycle, we further explored the role of ME2 K346 desuccinylation in the coordination of glycolysis and mitochondrial respiration by measuring the extracellular acidification rate (ECAR), lactate levels, oxygen consumption rate (OCR) and ATP levels. ME2 knockdown led to enhanced glycolysis and impaired mitochondrial respiration (Fig. 5I, J). Re-expression of ME2 K346R resulted in lower levels of glycolysis and stronger abilities to rescue impaired mitochondrial respiration compared with the effects of WT ME2 (Fig. 5I, J). Consistently, ME2 silencing resulted in elevated lactate levels and a reduction in ATP levels, which were rescued by the reintroduction of WT ME2 and ME2 K346R but not ME2 K346E (Fig. 5K, L). Moreover, ME2 K346R exerted a more profound rescuing effect than WT ME2 (Fig. 5K, L). Together, these data indicate that ME2 activated by K346 desuccinylation maintains the mitochondrial respiration rate in CRC cells.

ME2 K346 desuccinylation promotes tumor growth

We next examined the effect of ME2 K346 desuccinylation on cancer growth. As expected, ME2 depletion inhibited the cell proliferation and colony formation in HCT116 cells (Fig. 6A, B). HCT116 cells with the reconstituted expression of the K346R mutant but not the K346E mutant, exhibited greater proliferation and colony-forming capacity compared with the WT ME2 control group (Fig. 6A, B). In addition, we examined the clonal growth of cells under the condition of glutamine starvation. The ME2 K346R group showed decreased sensitivity to glutamine starvation, while the K346E group was more sensitive to glutamine deprivation compared with the WT ME2 group, indicating that cancer cells adapt to glutamine deprivation for survival by desuccinylating ME2 and thus increasing ME2 activity and cell survival (Fig. S3). These data demonstrate that ME2 K346 desuccinylation promotes CRC cell proliferation.

To further confirm the oncogenic role of ME2 K346 desuccinylation, we constructed mouse xenograft tumor models by subcutaneously injecting ME2-depleted HCT116 cells with reconstituted expression of WT ME2, ME2 K346R or ME2 K346E into athymic nude mice. The results showed that ME2 depletion inhibited tumor growth (Fig. 6C–G), and reduced the ratios of GSH/GSSG and $NADPH/NADP^+$ (Fig. 6H). Compared to WT ME2, the recombinant expression of ME2 K346R, but not ME2 K346E, showed greater rescuing effects on tumor growth and the ratios of GSH/GSSG and $NADPH/NADP^+$ (Fig. 6C–H). These results indicated that ME2 K346 desuccinylation promotes tumor growth in vivo.

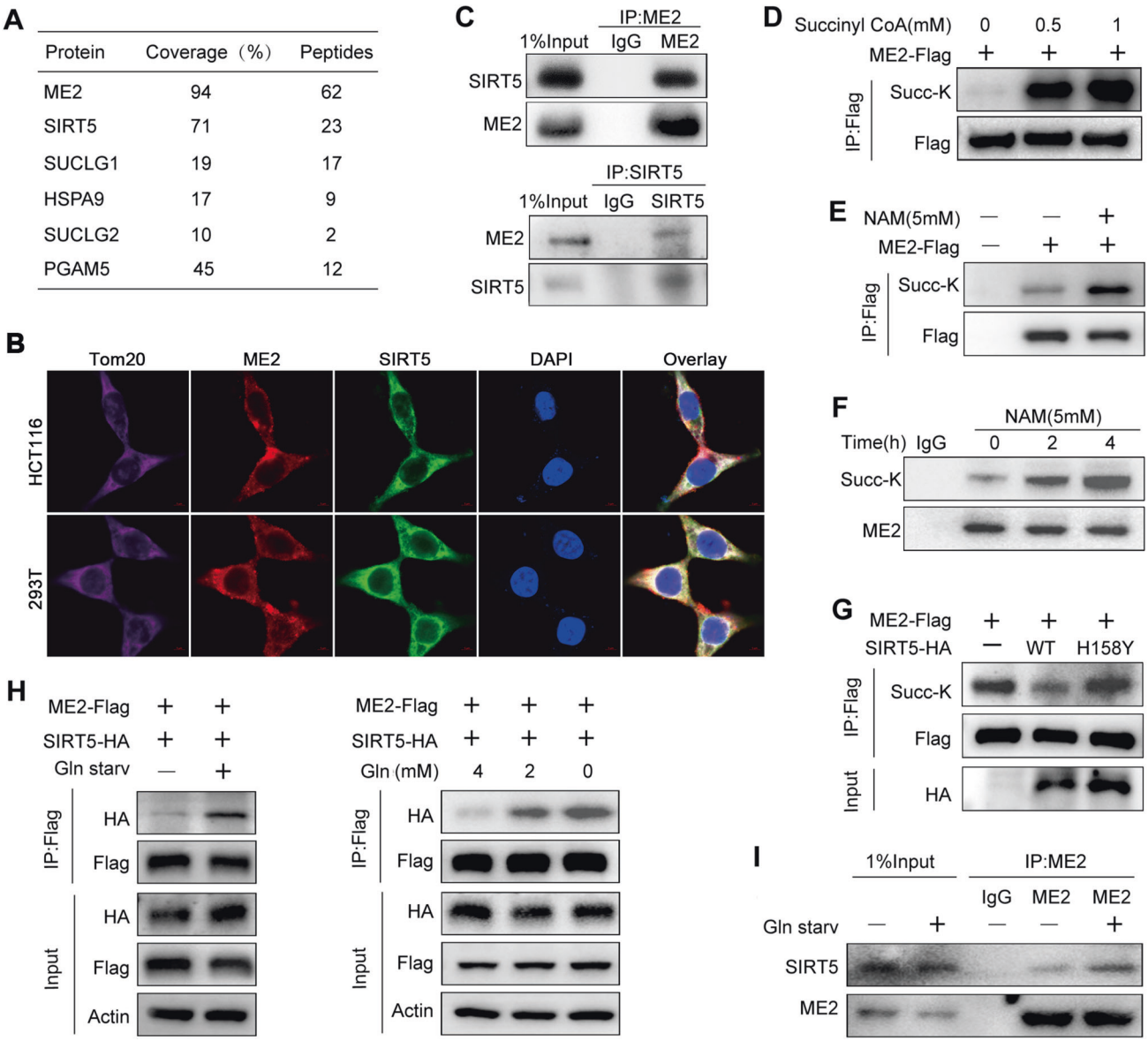

Fig. 2 SIRT5 interacts with and desuccinylates ME2. A Candidates of ME2-associated proteins identified by immunopurification and mass spectrometry analyses. **B** Immunofluorescence analyses of endogenous SIRT5, ME2 and the mitochondrial marker Tom20 in HEK293T and HCT116 cells. Scale bars, 5μm. **C** Endogenous interaction of SIRT5 and ME2 in HCT116 cells. **D** In vitro ME2 succinylation assay. ME2 proteins were incubated with different concentrations of succinyl-CoA. Protein succinylation levels were analyzed by western blotting. **E** Succinylation levels of ectopically expressed ME2 in HEK293T cells were measured. Cells were treated with 5 mM NAM for 3 h before harvesting. ME2-Flag was immunoprecipitated from cell lysates and its succinylation was examined with a pan-succinylated lysine antibody. **F** Succinylation levels of endogenous ME2 in HCT116 cells were analyzed. Cells were treated with 5 mM NAM for the indicated durations. Endogenous ME2 was immunoprecipitated and its succinylation was examined with a pan-succinylated lysine antibody. **G** Effects of SIRT5 or its dead mutant SIRT5 H158Y on the succinylation of ME2. **H** Effects of glutamine starvation on the interaction between ectopically expressed SIRT5 and ME2 in HEK293T cells. HEK293T cells transfected with Flag-tagged ME2 and HA-tagged SIRT5 were treated with glutamine (4 mM or indicated concentrations) for 6 h, followed by immunoprecipitation with anti-Flag M2 beads and analyses by western blotting. **I** Effects of glutamine starvation on the interaction between endogenous SIRT5 and ME2 in HCT116 cells. HCT116 cells were treated with glutamine (0 or 4 mM) for 6 h. Precipitated ME2 proteins were analyzed with anti-SIRT5 antibodies.

ME2 K346 succinylation levels are correlated with SIRT5 expression and prognosis in CRC

To determine the clinical relevance of SIRT5 and ME2 K346 succinylation, we performed IHC analyses with 146 primary CRC and adjacent NCTs with antibodies recognizing SIRT5 and succinylated ME2 K346 (Fig. 7A, B). We observed significantly lower levels of ME2 K346 succinylation and higher levels of SIRT5 in CRC tissues than in neighboring NCTs (Fig. 7C). In addition, the levels of ME2 K346 succinylation were negatively correlated with SIRT5 expression levels in CRC tissues (Fig. 7D). Moreover, low levels of ME2 K346 succinylation and high levels of SIRT5 in CRC tissues were associated with poor overall survival in CRC patients (Fig. 7E). These results support a crucial role for SIRT5-regulated ME2 K346 desuccinylation in predicting the prognosis of CRC patients.

DISCUSSION

ME2 is an NAD^+-dependent enzyme that links glycolysis and the TCA cycle through reversible oxidative decarboxylation of malate and pyruvate production, while producing large amounts of

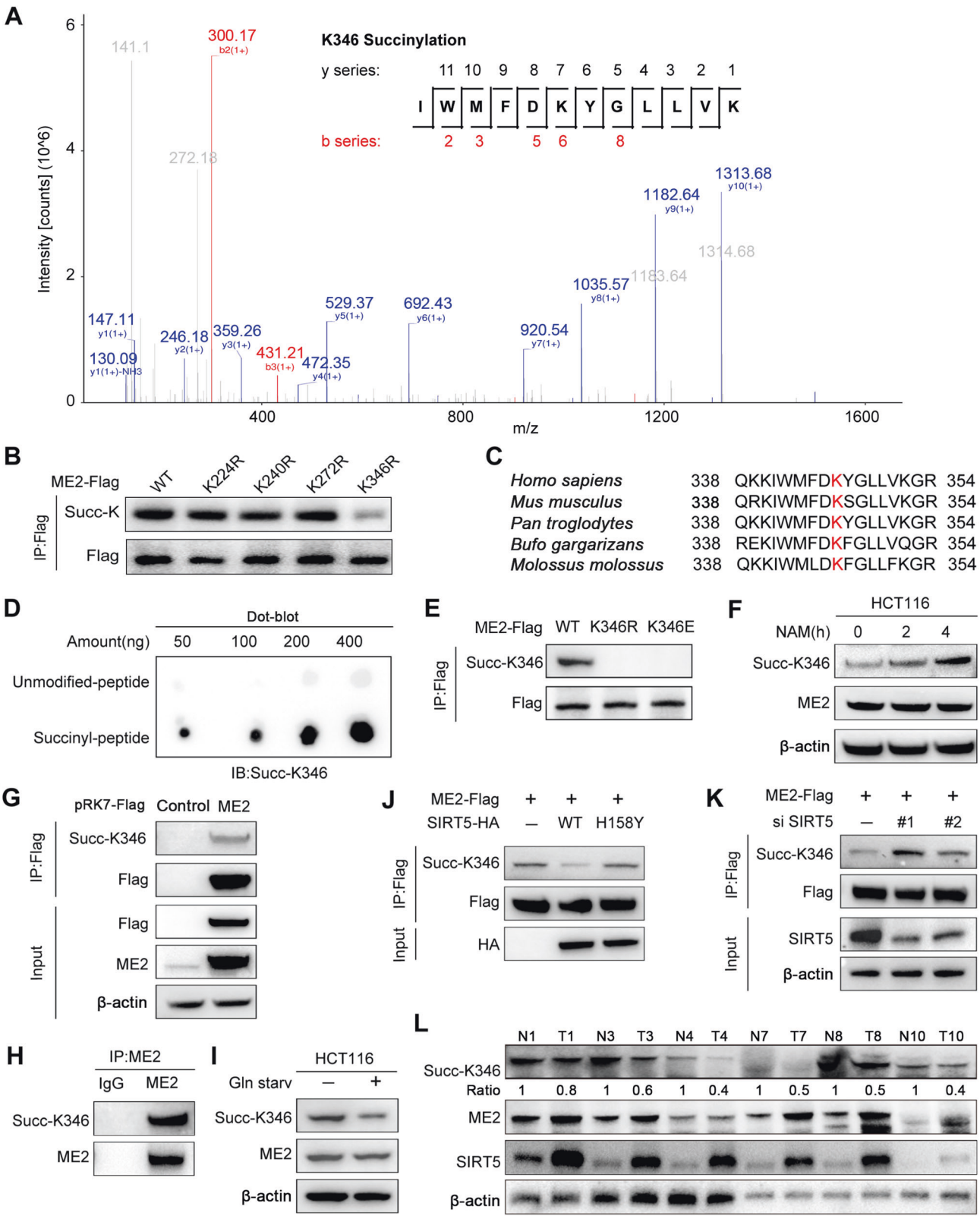

NADPH. A recent study revealed that ME2 promotes the synthesis of 2-HG, and elevated 2-HG in turn maintains the stability of mutant-p53, which promotes tumor development [16]. Notably, depletion of ME2, which impairs the NADPH production, conferred collateral lethality in pancreatic cancer [17]. In addition, inhibiting ME2 activity reduced cellular respiration and ATP synthesis [26]. Although ME2 has been reported to be involved in cancer development, the regulatory mechanism of ME2 functions in cancer, and whether it is post-translationally modified, remains poorly understood. In the present study, we showed that ME2 is overexpressed in CRC cells and promotes tumor growth. Importantly, we revealed that ME2 is succinylated at K346 and that SIRT5-mediated ME2 K346

Fig. 3 ME2 is succinylated at lysine 346. A Identification of succinylated peptides around ME2 K346 as determined by mass spectrometry. **B** Measurement of ME2 succinylation in HEK293T cells transfected with Flag-tagged wide-type (WT) or mutant (K224R, K240R, K272R and K346R) ME2. ME2-Flag was immunoprecipitated and its succinylation was examined with a pan-succinylated lysine antibody. **C** The K346 residue of ME2 (marked red) is evolutionarily conserved. **D** Characterization of the anti-Succ-K346 antibody using a dot blot assay. Nitrocellulose membranes were spotted with different amounts of succinyl-K346 peptide or unmodified peptide and immunoblotted with anti-Succ-K346 antibodies. **E** Validation of an anti-Succ-K346 antibody using western blotting. Succinylation levels of ME2-Flag WT, ME2-Flag K346R, or ME2-Flag K346E ectopically expressed in HEK293T cells were measured by the anti-Succ-K346 antibody. **F** Western blotting detection of the K346 succinylation levels of ME2 in HCT116 cells treated with 5 mM NAM. **G**, **H** Western blotting detection of the K346 succinylation levels of ectopically expressed ME2 (**G**) and endogenous ME2 (**H**) in HEK293T cells. **I** Western blotting analyses of K346 succinylation levels of HCT116 cells under the condition of glutamine starvation. **J** Effects of SIRT5 or its dead mutant SIRT5 H158Y on the succinylation of ME2 at K346. **K** Effects of SIRT5 knockdown on the succinylation of ME2 at K346. **L** Measurement of ME2 K346 succinylation, ME2, and SIRT5 protein levels in clinical CRC tissues (T) and adjacent normal tissues (N) using western blotting.

desuccinylation increases ME2 activity, leading to increased mitochondrial respiration and tumor growth.

Although aerobic glycolysis (the Warburg effect) is thought to be central to cancer cell metabolism, growing evidences support the idea that mitochondrial metabolism plays other important roles in addition to energy production, including ROS production, biosynthesis, and cell growth and death regulation, all of which are closely associated with tumorigenesis [5, 8]. In tumor cells, ME2 may act as a fumarate sensor; high fumarate levels promote the dimerization of ME2, which in turn enhances ME2 enzyme activity and promotes mitochondrial biosynthesis and cell proliferation [15]. In this study, we revealed that K346R mutant of ME2, which mimics the desuccinylated ME2, significantly increased the OCR and ATP levels and decreased the ECAR and lactate levels, implying that the desuccinylation of ME2 K346 leads to increased ME2 enzyme activity and thus enhances mitochondrial respiration in CRC cells. Correspondingly, ME2 K346R mutant increased the ratios of NADPH/$NADP^+$ and GSH/GSSG, and decreased the levels of ROS, highlighting the essential role of the SIRT5-ME2 axis in maintaining redox homeostasis and counteracting oxidative stress in tumor cells.

The levels of glucose and glutamine in the tumor microenvironment are dynamic, and cancer cells selectively use glucose and/or glutamine to maintain the TCA cycle function [28]. Interestingly, CRC cells are particularly dependent on glutamine metabolism and can consume glutamine to produce α-KG and thus replenish the TCA cycle [21, 24]. It has been shown that oncogenic PIK3CA mutations upregulate GPT2 expression and thus reprogram glutamine metabolism, explaining the dependence of CRC cells on glutamine metabolism [24]. These studies suggest that limiting the availability of glutamine may be a promising strategy for the treatment of cancers, especially CRC [24, 29, 30]. However, the multifaceted functions of mitochondria provide considerable flexibility for the growth and survival of tumor cells in hostile environments, including environments characterized by nutrient starvation, hypoxia, and drug therapy [31]. Glutamine starvation promotes MDH2 C138 palmitoylation and enhances its activity, thus accelerating mitochondrial respiration and ovarian cancer proliferation [32]. Glutamine deprivation can also cause elevated K388 acetylation of PGK1, which then binds and phosphorylates Beclin 1, ultimately initiating the formation of autophagosomes [33]. In this study, we reveal that glutamine deficiency promotes SIRT5-mediated ME2 K346 desuccinylation and increases its activity to enhance the TCA cycle. Intracellular glutamine is converted into α-KG, which then enters the TCA cycle and is transformed to succinyl-CoA in the subsequent step. Thus, our proposed mechanism implies a homeostatic feedback loop whereby intracellular accumulation of succinyl-CoA promotes K346 succinylation and reduces ME2 activity, delivering a signal that the TCA cycle is replete with needed substrates. In contrast, depletion of succinyl-CoA because of glutamine deprivation leads to desuccinylation and activation of ME2 and thus promotes mitochondrial respiration, supporting cancer growth.

Lysine succinylation is an evolutionarily conserved PTM and has been reported to affect the activity, stability and localization of multiple proteins, especially metabolic enzymes [20, 34–36]. In this study, we identified the residue K346 as the key succinylation site on ME2. Crystal structure analyses revealed that the K346 site is in front of a key channel for substrate and coenzyme NAD^+ entry. The succinylation modification of K346 changes the charge of the K346 site from positive to negative, thus blocking the affinity of ME2 for NAD^+ and substrates, both of which carry a negative charge, thereby decreasing the enzymatic activity of ME2. In addition, SIRT5, the only known desuccinylase located in mitochondria, is associated with metabolic disorders and cancer [20, 23, 37, 38]. Recent studies have shown that SIRT5 is highly expressed in CRC cells and activates GLUD1, thereby promoting glutamine catabolism and tumor cell proliferation [23]. However, SIRT5 may play a dual role in tumorigenesis by acting as both an oncogene and a tumor suppressor depending on its targets [23, 39]. We discover that SIRT5 catalyzes ME2 desuccinylation, leading to enhanced mitochondrial respiration and maintenance of redox homeostasis, ultimately promoting CRC tumor growth. Interestingly, SIRT5-regulated succinylation of ME2 is modulated by glutamine availability, which may be a compensatory response of CRC cells in response to glutamine starvation stimuli. Moreover, increased SIRT5 protein expression is associated with lower ME2 succinylation levels, further validating the role of the SIRT5-ME2 axis in promoting CRC tumor growth.

In this study, we revealed, for the first time, that ME2 is succinylated and discovered a previously unknown mechanism by which SIRT5 desuccinylates and activates ME2, which results in enhanced mitochondrial respiration and facilitates CRC tumor growth. Interestingly, the interaction of SIRT5 with ME2 is regulated by glutamine starvation, highlighting an important role for mitochondrial metabolism in sustaining tumor growth during nutrient deprivation. Given that ME2 is a promising target for cancer treatment [26, 40] and that ME2 K346 succinylation is associated with clinical outcomes of CRC patients, this study suggests that targeting the SIRT5-ME2 axis may be a new strategy for the treatment of CRC.

MATERIALS AND METHODS

Cell lines and clinical samples

CRC cell lines (HCT116, HCT8, RKO, SW480, SW620, and Caco2) were purchased from the American Type Culture Collection (ATCC). These cells were cultured in DMEM supplemented with 10% fetal bovine serum and 1% penicillin/streptomycin. All cell lines were authenticated by short tandem repeat (STR) profiling and tested as mycoplasma-free.

A total of 146 paired human CRC tissues and noncancerous tissues (NCTs) were collected at Affiliated Hospital of Jiangnan University. All participants gave written informed consent, and the local ethics committees approved the study. The studies were performed in accordance with the Declaration of Helsinki and International Ethical Guidelines for Biomedical Research Involving Human Subjects (CIOMS).

Reagents and antibodies

Anti-Flag M2 magnetic beads (A2220), succinyl CoA (S1129-5MG), and nicotinamide (NAM) (72345) were from Sigma. RPMI 1640 medium (without

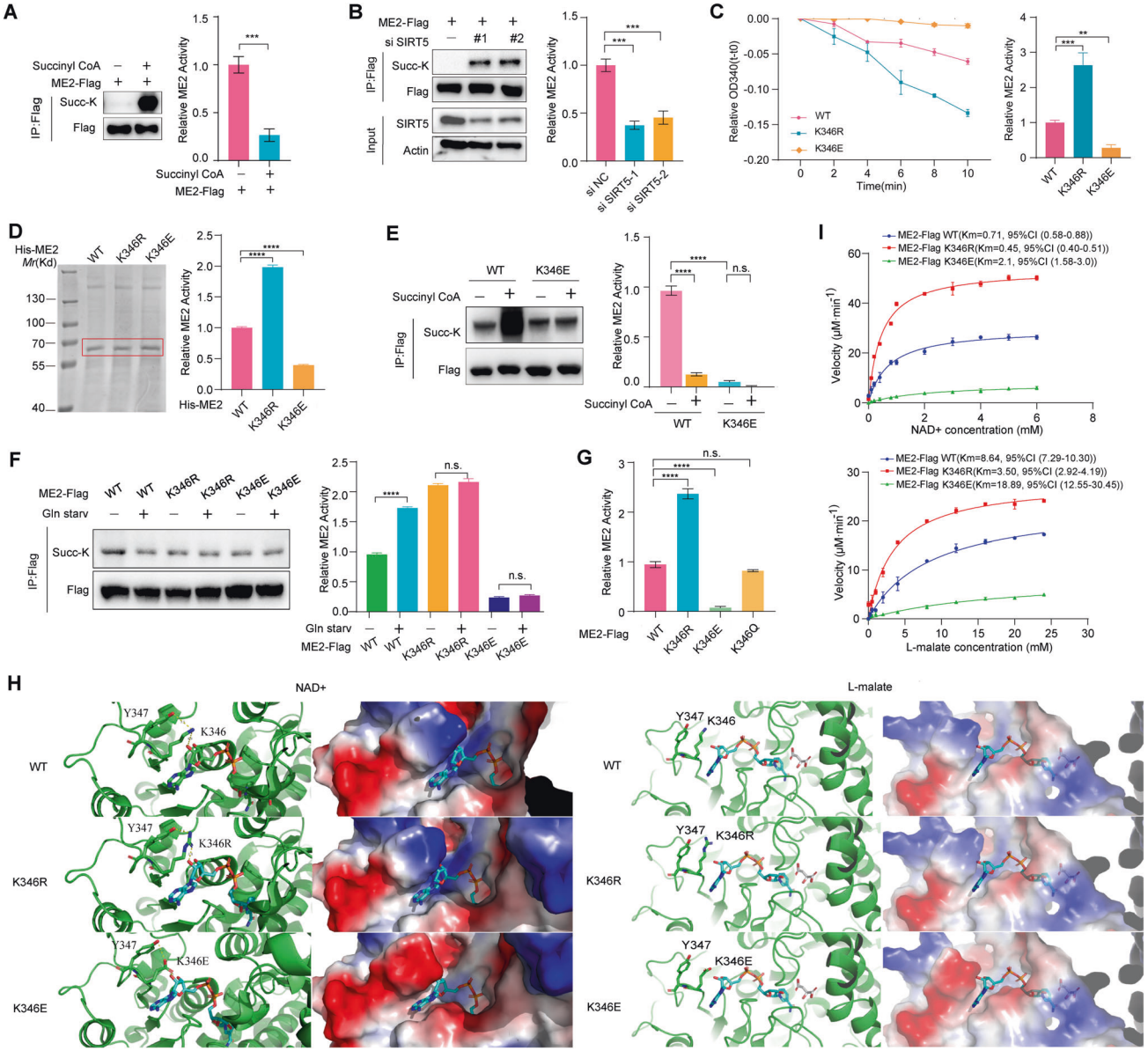

Fig. 4 Desuccinylation at K346 by SIRT5 enhances ME2 activity. A In vitro succinylation of ME2 decreased its activity. ME2 proteins were purified and incubated with or without 100 μM succinyl-CoA for 30 min at 37 °C before western blotting and ME2 enzymatic assays were performed. Unpaired two-tailed t-test was used for statistical analyses. **B** ME2 enzyme activity was determined after SIRT5 knockdown. Left, elevated ME2 succinylation after knockdown of SIRT5. Right, quantification of ME2 enzymatic activity. **C** K346R mutation increased ME2 activity. Different ME2 plasmids were transfected into HEK293T cells, and ME2 proteins were purified from these cells and subjected to ME2 enzymatic activity analyses. **D** Activity measurement of recombinant ME2 and its mutants. Recombinant ME2 and its mutated proteins were purified from *Escherichia coli*. SDS-PAGE, Coomassie Brilliant Blue staining, and ME2 activity assays were performed. **E** Succinyl-CoA decreased the enzymatic activity of ME2 WT but not that of the K346E mutant. HEK293T cells were transfected with the indicated plasmids, followed by immunoprecipitation and treatment with succinyl-CoA (100 μM, 30 min). Enzymatic activities of purified ME2 proteins were detected. **F**, **G** Effects of glutamine starvation (**F**) and K346Q (**G**) on the catalytic activities of ME2 and its mutants. Flag-tagged ME2 proteins were immunopurified from HEK293T cells transfected with different ME2 constructs and subjected to ME2 activity analyses. Cells were suffered from glutamine starvation for 6 h before harvesting (**F**). **H** Cartoon representation of the structure of human ME2 and its mutants. The NAD^+ binding pocket (left) and L-malate binding pocket (right) (PDB ID: 1EFK). ME2 proteins are depicted in light green, while the mutated positions are indicated by sticks. NAD^+ and L-malate molecules are also represented as sticks, with their carbon atoms colored cyan and white, respectively. The Y347 residue of ME2 is indicated by a stick representation. The right panels show the impact of K346R and K346E on the electrostatic environment surrounding the modified site. All figures were generated using PyMOL (www.pymol.org) **I** Steady-state kinetic analyses of WT ME2, ME2 K346R, and ME2 K346E. Recombinant proteins were purified and subjected to kinetic assays (NAD^+ and L-malate). Data are shown as mean ± S.D ($n = 3$). *P* values were calculated using Tukey's test (**E**, **F**) or Dunnett's test (**B**–**D** and **G**) after One-way ANOVA. **, $p < 0.01$; ***, $p < 0.001$; ****, $p < 0.0001$; n.s. not significant.

glutamine) (21870076) was from Thermo. 3×Flag peptides solution (P9801) and 6 × His peptide (P9811-5mg) were from Beyotime. Anti-His Tag Mouse mAb Agarose (ABT2053) was from Abbkine.

The antibodies were commercially obtained: β-actin antibody (81115-1-RR), HA antibody (51064-2-AP), ME2 antibody (24944-1-AP) and SIRT5 antibody (15122-1-AP) were from Proteintech. Flag antibody (M185-3) was from MBL. Pan-succinylation antibody (PTM-0401) was from PTM BIO. Succ-K346 antibody (4408-M-R1) was generated from YOUKE. Ki-67 antibody (GT209402) was from Gene Tech. Tom20 antibody (sc-17764) was from santa cruz.

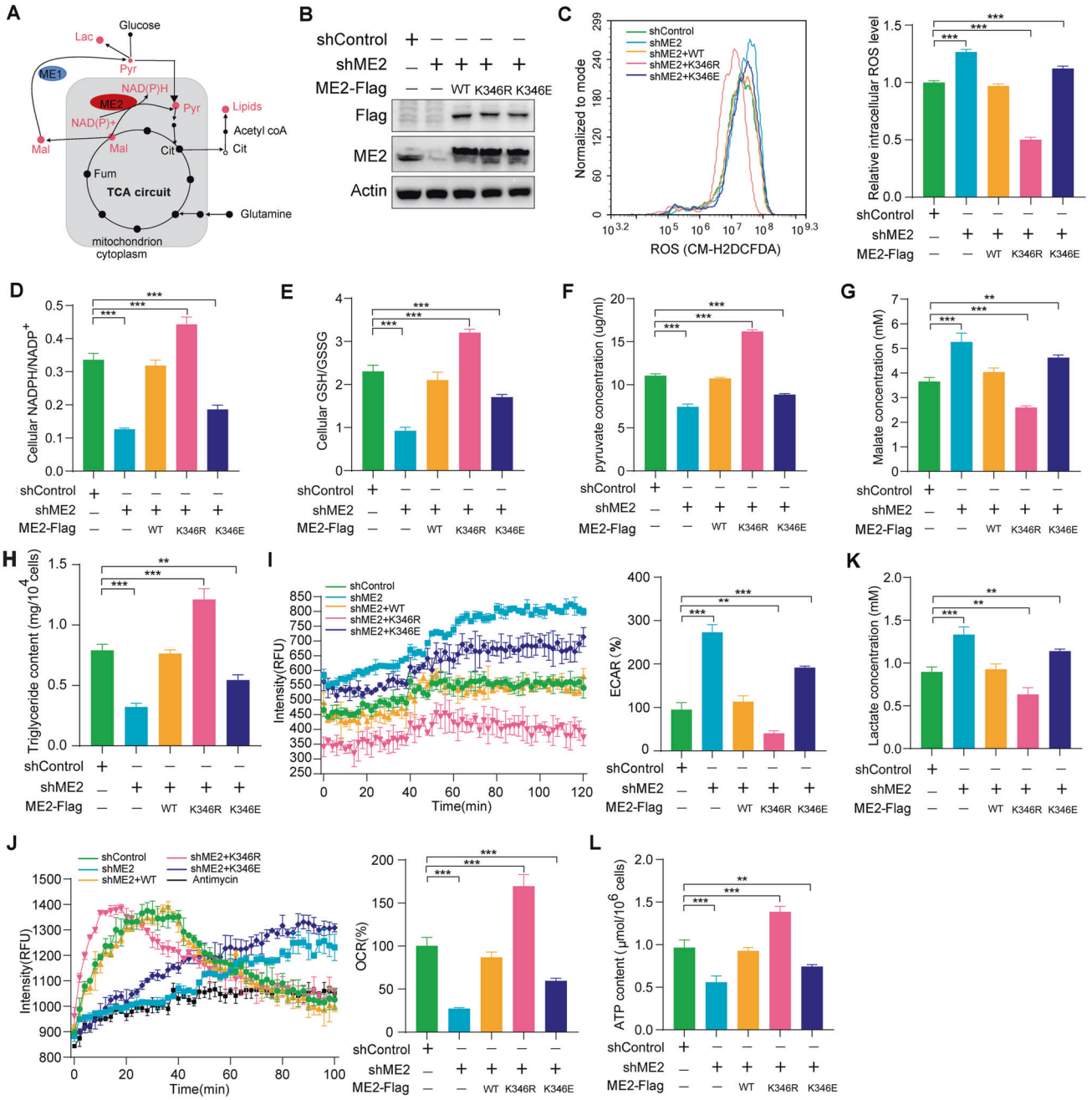

Fig. 5 ME2 K346 desuccinylation modulates mitochondrial respiration and redox homeostasis. A Schematic overview of malic enzymes involving in in central carbon metabolism. **B**–**H** Identification of reconstituted HCT116 cell lines with reconstituted protein expression. ME2-depleted HCT116 cells were reconstituted with empty vector, shRNA-resistant Flag-tagged WT, K346R, or K346E of ME2. Total cell lysates were prepared, and protein levels were measured by western blotting (**B**). ROS (**C**), NADPH/NADP$^+$ ratio (**D**) and GSH/GSSG ratio (**E**), pyruvate (**F**), malate (**G**) and triglyceride (**H**) were measured in the indicated cells were determined. **I**–**L** The ECAR (**I**), OCR (**J**), Lactate levels (**K**), and ATP production rate (**L**) in HCT116 cells with ME2–knockdown and re-expression were measured. *P* values were calculated using Dunnett's test after One-way ANOVA. **, $P < 0.01$; ***, $P < 0.001$; n.s., not significant.

Plasmid construction

The cDNA encoding full-length human ME2 was cloned into Flag-tagged vectors (pRK7-Flag). Point mutations in the ME2 constructs were generated using Site-Directed Mutagenesis kit (C215-01) purchased from Vazyme.

Oligonucleotides

The small interfering RNAs (siRNAs) of ME2 and SIRT5 were purchased from RiboBio (China) and the siRNA sequences are as follows: siSIRT5#1:5′-GCCCTT GAACATTTCCCAATG-3′; siSIRT5#2: 5′-GCATTAGAACTACAGACAAC-3′; siME2#1:5′-TATGGTTTATTAGTTAAGGGA-3′; siME2#2:5′-AGAGCCATGGCCTCTA TCAAT-3′. The shRNA targeting sequences: Human ME2 shRNA-1: 5′-AGTTCT TACAGAGCTACTAAA-3′; Human ME2 shRNA-2: 5′-GCACGGCTGAAGAAGCA TATA-3′.

Western blotting

Extracted proteins were separated by SDS-PAGE and transferred to a PVDF membrane blocked with 5% skim milk. Finally, the membrane was incubated with primary antibodies overnight. Visualization was performed using an ECL Kit (E412-02, Vazyme, China).

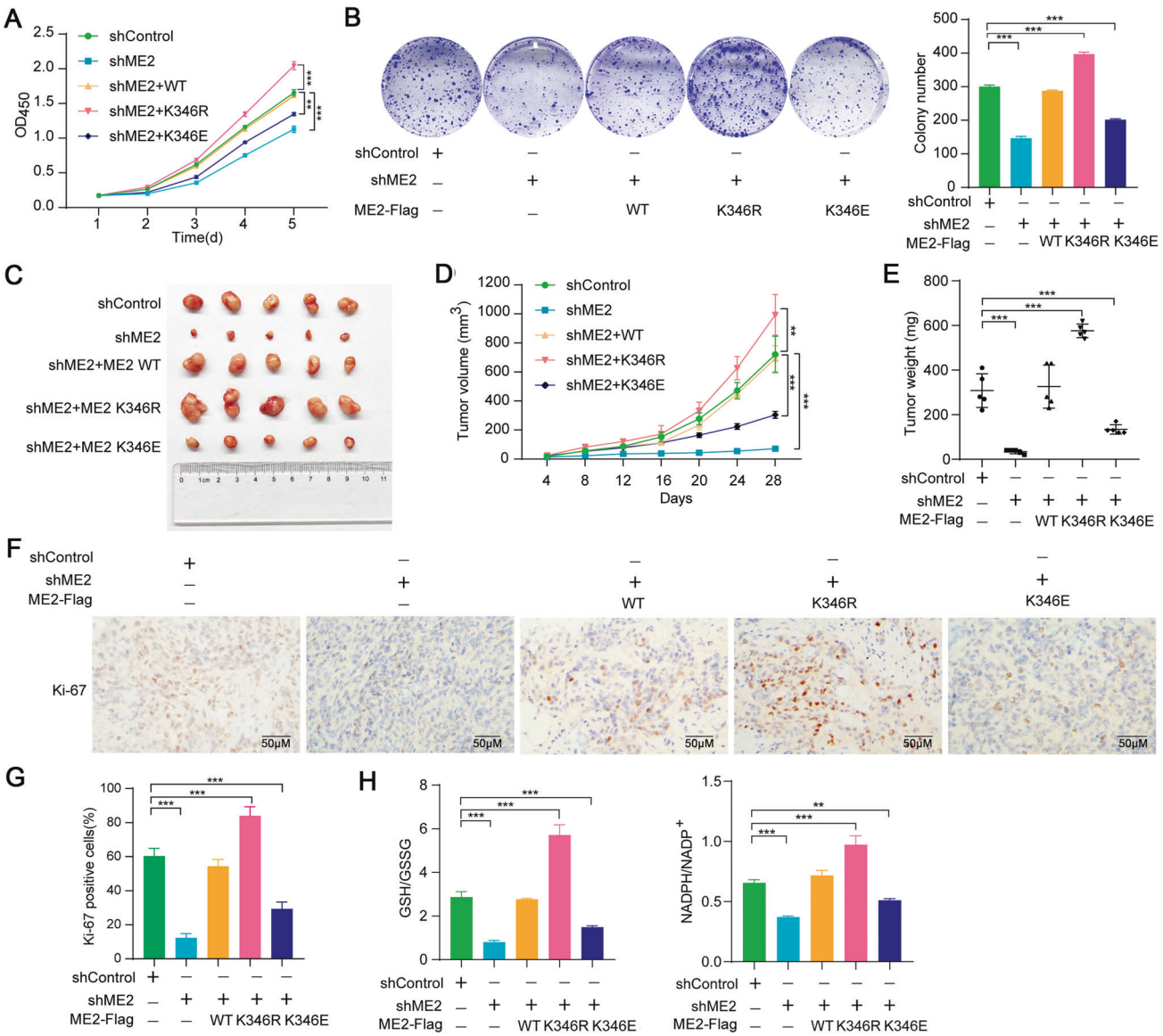

Fig. 6 ME2 K346 desuccinylation promotes tumor growth. A, **B** Cell proliferation (**A**) and colony formation assay results for the indicated HCT116 cells. **C**–**E** Effects of ME2 and its K346R or K346E mutants on the in vivo tumor growth. HCT116 cells (2×10^6) with different ME2 status were subcutaneously injected into the flanks of thymus-free nude mice ($n = 5$/group). The mice were euthanized and examined for tumor growth 28 days after injection (**C**). Tumor volumes (**D**) and tumor weights (**E**) were measured. **F**, **G** Ki67 expression in the xenograft tumors was measured by immunohistochemical staining. The number of Ki67-positive cells in 10 microscopic fields were counted. The magnification is 20×. Scale bars, 50 μm. **H** Measurements of the GSH/GSSG (**G**) and NADPH/$NADP^+$ ratios (**H**) in the xenograft tumor tissues. *P* values were calculated using Dunnett's test after One-way ANOVA. **, $P < 0.01$; ***, $P < 0.001$; n.s., not significant.

Immunohistochemistry (IHC) staining and scoring

Human CRC tissues were stained with antibodies against ME2, SIRT5, and ME2 K346succ. We sectioned paraffin-embedded tissues at 4 μm and then incubated these slides with corresponding antibodies at 4 °C overnight. The following steps were in accordance with the protocols provided by the manufacturer of GTVision III Detection System/Mo&Rb (Gene Tech, China). In addition, sections of paraffin-embedded xenograft tissues were stained with anti-Ki67 antibodies. Staining results were assessed by two independent authors blinded to the patients' clinicopathological data.

Cell proliferation and colony formation assays

A total of 2000–3000 cells were plated in 96-well plates and cultured for 5 days. CCK-8 assays were performed to measured cell proliferation according to the manufacturer's instructions. To perform the colony formation assay, 1000–1500 cells were seeded into six-well plates and cultured for approximately 14 days. Cell colonies were fixed with 4% formaldehyde and stained with 0.1% crystal violet for 10 min, and the number of colonies was counted.

Co-immunoprecipitation (Co-IP)

Cells were lysed in NP40 lysis buffer (50 mM Tris-HCl, pH 7.5, 150 mM NaCl, 0.1%–0.5% NP40, 1 mM PMSF, and related protease inhibitors). Co-IP assays were performed by incubating anti-Flag M2 magnetic beads (A2220, Sigma, USA) at 4 °C for over 4 h. After incubation, the beads were washed three times with ice-cold NP40 buffer, and the proteins were eluted in 1×loading buffer by heating at 100 °C for 10 min. Finally, the eluted proteins were analyzed by western blotting.

Immunofluorescence (IF) analyses

According to standard protocols, cells were fixed and incubated with primary antibodies (at a 1:100 dilution), fluorescence dye-conjugated secondary antibodies, and DAPI. Immunofluorescence images of the cells were observed and captured using confocal microscopy.

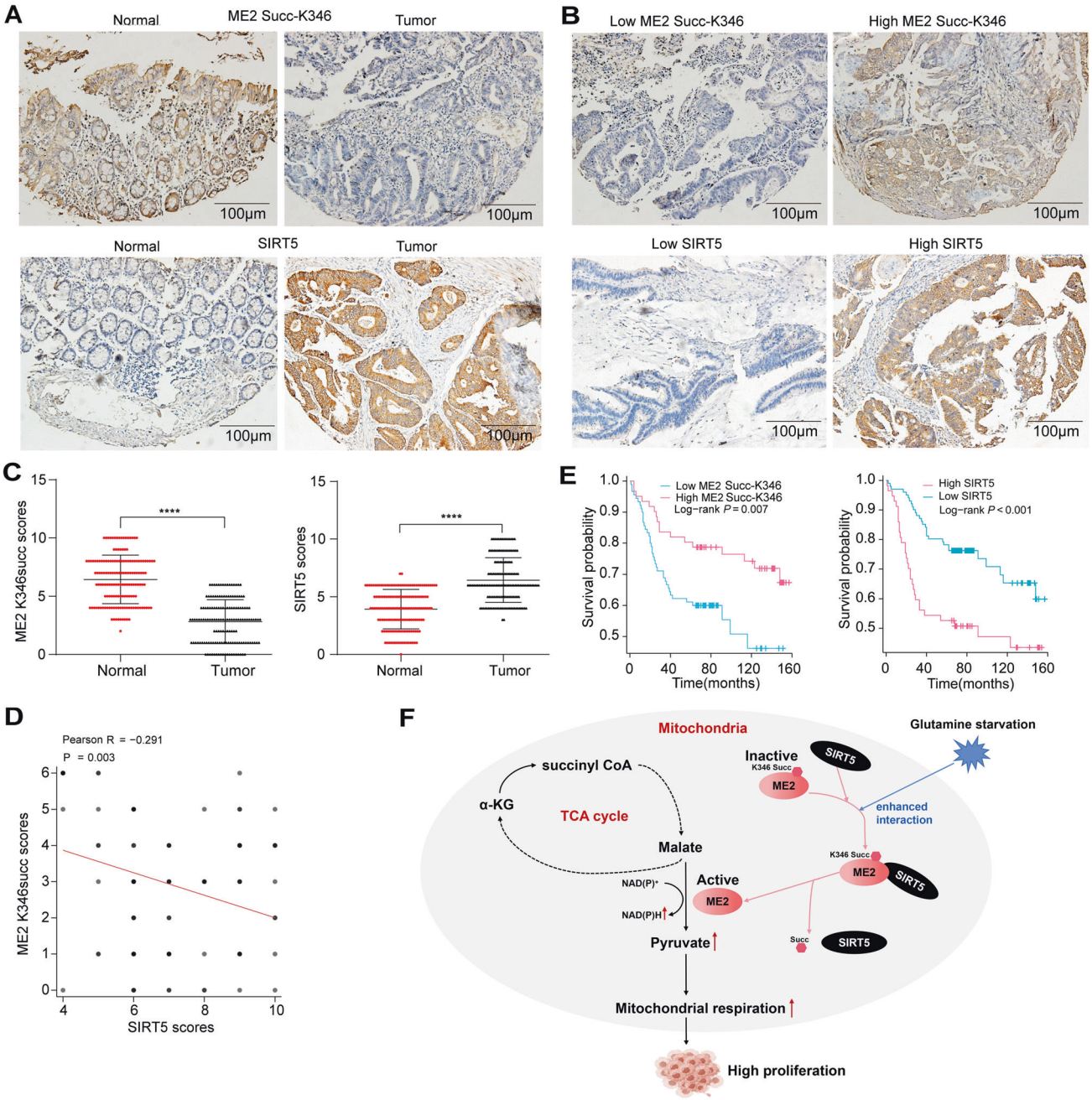

Fig. 7 ME2 K346 succinylation and SIRT5 are aberrantly expressed in CRC tissues. A–C The levels of ME2 K346 succinylation and SIRT5 in146 paired CRC tissues and their paired adjacent normal tissues were measured by immunohistochemistry staining. Representative staining images and scores for ME2 K346 succinylation (**A** and **C**) and SIRT5 (**B** and **C**) are shown. Scale bars, 100 μM. Mann-Whitney U Test was used for statistical analyses for (**C**). ****, $P < 0.0001$. **D** The correlation between ME2 K346succ expression and SIRT5 levels was analyzed. **E** Kaplan-Meier survival analyses based on the succinylation levels of ME2 K346 and SIRT5 expression in CRC tissues. *P* values were calculated using the log-rank test. **F** A regulatory mechanism underlying SIRT5-coupled ME2 desuccinylation and activation under glutamine deprivation conditions. ME2 is succinylated at K346, leading to decreased ME2 enzymatic activity. The interaction between SIRT5 and ME2, which is facilitated by glutamine starvation, leads to K346 desuccinylation and increased ME2 enzymatic activity. Activated ME2 enhances mitochondrial respiration and promotes tumor growth.

Generation of reconstituted HCT116 cell lines

To deplete endogenous ME2, the shRNA targeting sequence was inserted into pLKO.1 retroviral vector (pLKO-shME2). We then cloned shRNA-resistant Flag-tagged WT or K346R/K346E ME2 into the retroviral vector pQCXIH. Recombinant retrovirus was packaged with the plasmids constructed by Shanghai GenePharma Co., Ltd. (Shanghai, China). Concentrated viruses infect 5×10^5 cells in a 60 mm dish pretreated with 10 mg/mL polybrene. Stably expressing shME2 was screened with 250 μg/mL hygromycin for 2 weeks. Stably expressing shRNA-resistant Flag-tagged ME2 WT, K346R, and K346E were screened with 2 μg/mL puromycin for 2 weeks. The efficiencies of knockdown or overexpression were tested by western blotting.

Mass spectrometry analyses

Total cell lysates of HEK293T cells transfected with ME2-Flag were incubated with anti-flag M2 magnetic beads for more than 4 h at 4 °C. The protein-bead complexes were washed three times with ice-cold NP40

buffer. The proteins were then eluted from beads by incubating 3× Flag peptides solution (P9801, Beyotime, China) at 4 °C for 2 h. Finally, total eluted proteins were analyzed by mass spectrometry in PTM Biolabs (Hangzhou, China).

Expression and purification of recombinant human ME2

The plasmids pRH281-ME2 K346R and K346E mutants were generated using Site-Directed Mutagenesis kit (C215-01, Vazyme, China). The protein was expressed in Escherichia coli BL21 (DE3) cells, and a single colony was selected and cultured in LB medium in the presence of ampicillin (100 mg/L) at 37 °C with agitation at 200 rpm. Protein expression was induced at 18 °C by 400 µmol/L of 3-Indoleacrylic acid when the cultures reached an optical density of 0.4–0.6 at 600 nm (OD_{600}). After 10 h of induction, the cells were harvested and lysed. After centrifugation at 12,000 rpm for 30 min, the supernatants were collected and incubated with His beads for 5 h at 4 °C. Finally, the bound proteins were eluted with 6× His peptide at 4 °C for 2 h and concentrated by ultrafiltration.

Measurement of ME2 activity

The purified ME2 or its mutant protein samples were added to the enzyme reaction mixtures that contained 50 mmol/L MES (pH = 6.5), 10 mmol/L $MgCl_2$, 24 mmol/L L-malate, and 1 mmol/L NAD^+. The monitored increase in the absorbance at 340 nm (NADPH production) was used to calculate ME2 activity. All assays were carried out at 30 °C, and the absorbance was measured by an EPOCH2 microplate reader (BioTek).

Calculation of the K_m of ME2

To calculate the Km of NAD+, a total of 10 nmol/L prokaryotic purified ME2 were added to the enzyme reaction mixtures that contained different concentrations of NAD+. To determine the Km of L-malate, the enzyme reaction mixtures contained different concentrations of L-malate. For all reactions, the absorbance at 340 nm was monitored for 5 min using an EPOCH2 microplate reader (BioTek). Michaelis-Menten equation was used to estimate Km.

Measurement of intracellular NADPH/$NADP^+$ and GSH/GSSG

Cells were seeded into 6-well plates and incubated for 24 h before cell harvesting. The cellular GSH/GSSG ratios or NADPH/$NADP^+$ ratios of these cells were analyzed spectrophotometrically by using a GSH and GSSG Assay Kit (S0053, Beyotime) or an NADPH/$NADP^+$ Assay Kit (S0179, Beyotime) according to the manufacturer's instructions.

Measurement of intracellular pyruvate, malate, triglyceride, lactate, and ATP levels

Cells were plated in a 96-well plate and incubated for 24 h. According to the manufacturer's instructions, intracellular pyruvate, malate, triglyceride, lactate, or ATP levels were measured spectrophotometrically by using a Pyruvate (PA) Content Assay Kit (BC2205, Solarbio), Malic Acid Content Assay kit (BC5495, Solarbio), Triglyceride (TG) Content Assay Kit (BC0625, Solarbio), L-Lactic Acid Colorimetric Assay Kit (E-BC-K044-M, Eton) and ATP Content Assay Kit (BC0305, Solarbio), respectively.

Measurement of ECAR

ECAR was analyzed using the pH-sensitive BBcellProbe P61 fluorescent probe supplied by the ECAR assay kit (BB-48311, BestBio). Cells were seeded in a 96-well clear-flat-bottom black microplate and incubated for 2 d. The BBcellProbe P61 probe was then added to the cells. The plate was read on an EPOCH2 microplate reader (BioTek) in kinetic mode at 37 °C for 2 h (1 read per 3 min, Ex 488/Em 580). ECAR was calculated from the slope of the kinetic curve according to the manufacturer's instructions.

Measurement of OCR

OCR was measured with the Oxygen Consumption Rate kit (600800, Cayman Chemical). Cells were seeded in a 96-well clear-flat-bottom black microplate and incubated for 2 d. After adding the Phosphorescent Oxygen probe to the wells, 100 µL mineral oil was added to each well on top of the medium. The plate was read on an EPOCH2 microplate reader (BioTek) in kinetic mode at 37 °C for 2 h (1 read per 3 min, Ex 380/Em 650). Basal OCR levels of the cells were calculated from the slope of the kinetic curve following the manufacturer's instructions.

Intracellular reactive oxygen species (ROS) assay

According to the manufacturer's instructions, intracellular ROS levels were determined using the Reactive Oxygen Species Assay Kit (S0033, Beyotime). Briefly, cells were inoculated into 6-well plates and cultured for 48 h. Afterward, H2DCF-DA (10 µM) was added to the culture and incubated for 20 min at 37 °C. Finally, all cells were analyzed by FACS analysis (BD, United States).

Identification of ME2 acetylation sites

HEK293T cells were transfected with Flag-tagged ME2 for 48 h. Cells were treated with 5 mM nicotinamide (NAM, 72345, Sigma, USA) for 6 h before harvesting. Total cells lysates were incubated with Flag (M2) magnetic beads for over 4 h, and the protein-bead complexes were washed three times with ice-cold NP40 buffer. The proteins were then eluted from beads by incubating 3× Flag peptides solution (P9801, Beyotime) at 4 °C for 2 h. Eluted proteins were separated by SDS-PAGE and stained with Coomassie Brilliant Blue. The expected protein bands were then excised at 55–70 kD and analyzed by mass spectrometry in PTM Biolabs (Hangzhou, China).

Tumor formation assays in nude mice

ME2-depleted HCT116 cells or HCT116 cells stably expressing ME2 (ME2 WT, ME2 K346R, and ME2 K346E) were subcutaneously injected into the same flank of athymic male BALB/c nude mice obtained from Cavens Biogle (Changzhou, China) at 5 weeks of age (n = 5 for each group). The mice were sacrificed 3 weeks after injection, and tumor growth was measured. The mice were randomly divided to groups to minimize the effects of small differences between them.

Statistical analyses

Data are expressed as the mean ± SD and analyzed with a two-tailed Student's t-test or one-way analysis of variance (ANOVA). The Kaplan-Meier method and log-rank test were used to assess and compare group survival. Univariate and multivariate Cox proportional hazards regression models were performed to explore independent prognostic factors. All statistical analyses were performed using SPSS 20.0 software (IBM, SPSS, USA) and a level of *P* value less than 0.05 was considered statistically significant.

DATA AVAILABILITY

The full and uncropped western blots were uploaded as the Supplemental Material. Other datasets used and/or analyzed during the study are available from the corresponding author on reasonable request.

REFERENCES

1. Pavlova NN, Zhu J, Thompson CB. The hallmarks of cancer metabolism: Still emerging. Cell Metab. 2022;34:355–77.
2. Xu D, Shao F, Bian X, Meng Y, Liang T, Lu Z. The evolving landscape of non-canonical functions of metabolic enzymes in cancer and other pathologies. Cell Metab. 2021;33:33–50.
3. Zhao J, Zhang J, Yu M, Xie Y, Huang Y, Wolff DW, et al. Mitochondrial dynamics regulates migration and invasion of breast cancer cells. Oncogene. 2013;32:4814–24.
4. Kashatus JA, Nascimento A, Myers LJ, Sher A, Byrne FL, Hoehn KL, et al. Erk2 phosphorylation of Drp1 promotes mitochondrial fission and MAPK-driven tumor growth. Mol Cell. 2015;57:537–51.
5. Weinberg SE, Chandel NS. Targeting mitochondria metabolism for cancer therapy. Nat Chem Biol. 2015;11:9–15.
6. Li Y, Bie J, Zhao L, Song C, Zhang T, Li M, et al. SLC25A51 promotes tumor growth through sustaining mitochondria acetylation homeostasis and proline biogenesis. Cell Death Differ. 2023;30:1916–30.
7. Sedlak JC, Yilmaz OH, Roper J. Metabolism and colorectal cancer. Annu Rev Pathol. 2023;18:467–92.
8. Sainero-Alcolado L, Liano-Pons J, Ruiz-Perez MV, Arsenian-Henriksson M. Targeting mitochondrial metabolism for precision medicine in cancer. Cell Death Differ. 2022;29:1304–17.
9. Spinelli JB, Haigis MC. The multifaceted contributions of mitochondria to cellular metabolism. Nat Cell Biol. 2018;20:745–54.
10. Martinez-Outschoorn UE, Peiris-Pages M, Pestell RG, Sotgia F, Lisanti MP. Cancer metabolism: a therapeutic perspective. Nat Rev Clin Oncol. 2017;14:11–31.
11. Wei Z, Song J, Wang G, Cui X, Zheng J, Tang Y, et al. Deacetylation of serine hydroxymethyl-transferase 2 by SIRT3 promotes colorectal carcinogenesis. Nat Commun. 2018;9:4468.

12. Qiao S, Lu W, Glorieux C, Li J, Zeng P, Meng N, et al. Wild-type IDH2 protects nuclear DNA from oxidative damage and is a potential therapeutic target in colorectal cancer. Oncogene. 2021;40:5880–92.
13. Liu L, Qi L, Knifley T, Piecoro DW, Rychahou P, Liu J, et al. S100A4 alters metabolism and promotes invasion of lung cancer cells by up-regulating mitochondrial complex I protein NDUFS2. J Biol Chem. 2019;294:7516–27.
14. Jiang P, Du W, Mancuso A, Wellen KE, Yang X. Reciprocal regulation of p53 and malic enzymes modulates metabolism and senescence. Nature. 2013;493:689–93.
15. Wang YP, Sharda A, Xu SN, van Gastel N, Man CH, Choi U, et al. Malic enzyme 2 connects the Krebs cycle intermediate fumarate to mitochondrial biogenesis. Cell Metab. 2021;33:1027–1041.e8.
16. Zhao M, Yao P, Mao Y, Wu J, Wang W, Geng C, et al. Malic enzyme 2 maintains protein stability of mutant p53 through 2-hydroxyglutarate. Nat Metab. 2022;4:225–38.
17. Dey P, Baddour J, Muller F, Wu CC, Wang H, Liao WT, et al. Genomic deletion of malic enzyme 2 confers collateral lethality in pancreatic cancer. Nature. 2017;542:119–23.
18. Yang Y, Zhang Z, Li W, Si Y, Li L, Du W. alphaKG-driven RNA polymerase II transcription of cyclin D1 licenses malic enzyme 2 to promote cell-cycle progression. Cell Rep. 2023;42:112770.
19. Yang Y, Gibson GE. Succinylation Links Metabolism to Protein Functions. Neurochem Res. 2019;44:2346–59.
20. Yang X, Wang Z, Li X, Liu B, Liu M, Liu L, et al. SHMT2 desuccinylation by SIRT5 drives cancer cell proliferation. Cancer Res. 2018;78:372–86.
21. Tong Y, Guo D, Lin SH, Liang J, Yang D, Ma C, et al. SUCLA2-coupled regulation of GLS succinylation and activity counteracts oxidative stress in tumor cells. Mol Cell. 2021;81:2303–16 e8.
22. Li W, Kou J, Zhang Z, Li H, Li L, Du W. Cellular redox homeostasis maintained by malic enzyme 2 is essential for MYC-driven T cell lymphomagenesis. Proc Natl Acad Sci USA. 2023;120:e2217869120.
23. Wang YQ, Wang HL, Xu J, Tan J, Fu LN, Wang JL, et al. Sirtuin5 contributes to colorectal carcinogenesis by enhancing glutaminolysis in a deglutarylation-dependent manner. Nat Commun. 2018;9:545.
24. Hao Y, Samuels Y, Li Q, Krokowski D, Guan BJ, Wang C, et al. Oncogenic PIK3CA mutations reprogram glutamine metabolism in colorectal cancer. Nat Commun. 2016;7:11971.
25. Verdin E, Ott M. 50 years of protein acetylation: from gene regulation to epigenetics, metabolism and beyond. Nat Rev Mol Cell Biol. 2015;16:258–64.
26. Hsieh JY, Chen KC, Wang CH, Liu GY, Ye JA, Chou YT, et al. Suppression of the human malic enzyme 2 modifies energy metabolism and inhibits cellular respiration. Commun Biol. 2023;6:548.
27. Zhu Y, Gu L, Lin X, Liu C, Lu B, Cui K, et al. Dynamic regulation of ME1 Phosphorylation and Acetylation Affects Lipid Metabolism and Colorectal Tumorigenesis. Mol Cell. 2020;77:138–49.e5.
28. Yang C, Ko B, Hensley CT, Jiang L, Wasti AT, Kim J, et al. Glutamine oxidation maintains the TCA cycle and cell survival during impaired mitochondrial pyruvate transport. Mol Cell. 2014;56:414–24.
29. Altman BJ, Stine ZE, Dang CV. From Krebs to clinic: glutamine metabolism to cancer therapy. Nat Rev Cancer. 2016;16:619–34.
30. Edwards DN, Ngwa VM, Raybuck AL, Wang S, Hwang Y, Kim LC, et al. Selective glutamine metabolism inhibition in tumor cells improves antitumor T lymphocyte activity in triple-negative breast cancer. J Clin Invest. 2021;131:e140100.
31. Vyas S, Zaganjor E, Haigis MC. Mitochondria and cancer. Cell. 2016;166:555–66.
32. Pei X, Li KY, Shen Y, Li JT, Lei MZ, Fang CY, et al. Palmitoylation of MDH2 by ZDHHC18 activates mitochondrial respiration and accelerates ovarian cancer growth. Sci China Life Sci. 2022;65:2017–30.
33. Qian X, Li X, Cai Q, Zhang C, Yu Q, Jiang Y, et al. Phosphoglycerate kinase 1 phosphorylates Beclin1 to induce autophagy. Mol Cell. 2017;65:917–931.e6.
34. Wang X, Shi X, Lu H, Zhang C, Li X, Zhang T, et al. Succinylation inhibits the enzymatic hydrolysis of the extracellular matrix protein fibrillin 1 and promotes gastric cancer progression. Adv Sci. 2022;9:e2200546.
35. Lin ZF, Xu HB, Wang JY, Lin Q, Ruan Z, Liu FB, et al. SIRT5 desuccinylates and activates SOD1 to eliminate ROS. Biochem Biophys Res Commun. 2013;441:191–5.
36. Qi H, Ning X, Yu C, Ji X, Jin Y, McNutt MA, et al. Succinylation-dependent mitochondrial translocation of PKM2 promotes cell survival in response to nutritional stress. Cell Death Dis. 2019;10:170.
37. Wang K, Hu Z, Zhang C, Yang L, Feng L, Yang P, et al. SIRT5 contributes to colorectal cancer growth by regulating T cell activity. J Immunol Res. 2020;2020:3792409.
38. Liu X, Rong F, Tang J, Zhu C, Chen X, Jia S, et al. Repression of p53 function by SIRT5-mediated desuccinylation at Lysine 120 in response to DNA damage. Cell Death Differ. 2022;29:722–36.
39. Hu T, Shukla SK, Vernucci E, He C, Wang D, King RJ, et al. Metabolic Rewiring by Loss of Sirt5 Promotes Kras-Induced Pancreatic Cancer Progression. Gastroenterology. 2021;161:1584–600.
40. Sarfraz I, Rasul A, Hussain G, Hussain SM, Ahmad M, Nageen B, et al. Malic enzyme 2 as a potential therapeutic drug target for cancer. IUBMB Life. 2018;70:1076–83.

ACKNOWLEDGEMENTS

We thank Professor Li Jia (Shanghai Institute of Materia Medica, Chinese Academy of Sciences) for providing the pRH-ME2 plasmids. We also thank Professor Yu Wei (Fudan University) for providing the SIRT5-HA and SIRT5-HA H158Y plasmids. This work was supported by the Natural Science Foundation of China (82002964, 82173063), China Postdoctoral Science Foundation (2022M711370), Wuxi Taihu Lake Talent Plan for Leading Talents in Medical and Health Profession, Wuxi Medical Key Discipline (ZDXK2021002) and Youth Program of Wuxi Medical Foundation (Q202123).

AUTHOR CONTRIBUTIONS

CL, PT, and ZH designed the research. CL and PT performed most of the experiments. KC performed bioinformatic analyses. SY and BF collected clinical samples. ZH and CL supervised the project. CL, PT, FL, and ZH wrote the manuscript.

COMPETING INTERESTS

The authors declare no competing interests.

ETHICS APPROVAL

All animal experiments were performed in accordance with the National Institutes of Health Guide for Care and Use of Laboratory Animals and were approved by the Clinical Research Ethics Committees of Jiangnan University (JN. No20220515b0320730[151]).

ADDITIONAL INFORMATION

Supplementary information The online version contains supplementary material available at https://doi.org/10.1038/s41418-023-01240-y.

Correspondence and requests for materials should be addressed to Chaoqun Li or Zhaohui Huang.